

## Face Detection In Color Images Using Pixel-based Skin Color Detection Techniques

Ravi Subban<sup>1</sup>, Krishnan Nallaperumal<sup>2</sup>

### ABSTRACT

The selection of the best color space for skin detection in color images is important in many computer vision areas and this paper presents a comparative study on the pixel-based skin color detection techniques. Three main issues of the face detection are the selection of the best color space, skin color pixel classification algorithm and face detection algorithm. A large set of XM2VTS face database is used to examine whether the selection of color space can enhance the compactness of the skin class and discriminability between skin and non-skin class in thirteen color spaces, six different skin color pixel classification algorithms and one face detection algorithm. The results show that 1) the selection of the color space can improve the skin classification performance 2) the segmentation performance degrades only when chrominance information is used for classification 3) Bayesian classifier is found to perform better as compared to other classification algorithms, like Gaussian classifiers. Piece-wise linear decision boundary classifier algorithm outperforms all the other skin classification algorithms when used for images with good illumination conditions. The template matching technique is used to mark the face region in the image.

---

<sup>1</sup>Selection Grade Lecturer, Centre for Information Technology and Engineering, Manonmaniam Sundaranar University, Tirunelveli - 627012, Tamilnadu, India. Phone : +91-462-2323650; Fax : +91-462-2334363; email : subban\_ravi@yahoo.co.in.

<sup>2</sup>Professor and Head, Centre for Information Technology and Engineering, Manonmaniam Sundaranar University, Tirunelveli - 627012, India. Phone:+91-462-2323650; Fax: +91-462-2334363; email: krishnancite@ieee.org.

### 1. INTRODUCTION

DETECTING human face regions in an image is the paramount importance in many computer vision areas like face detection, face recognition, and video surveillance [1], [2], [3]. The face detection techniques involve the classification of each image pixel into skin and non-skin categories on the basis of pixel color [4], [5], [6]. The reason for using pixel color to detect human face skin is that the human face skin has very consistent colors which are distinct from the colors of other objects. Color is a powerful cue that can be used as a first step in skin detection because of its advantages: low computational cost, robustness against illumination changing and geometrical transformation.

When building a system that uses skin color as a feature for face detection, two issues must be addressed: what color space to select, which color skin classification algorithm to use. This paper covers both of the questions. In the past few years, a number of comparative studies of skin color pixel classification have been reported. Jones and Rehg [10] used the Bayesian classifier with the histogram technique for skin detection. Terrillon et al. [8] compared Gaussian and Gaussian mixture models across nine chrominance spaces. Phung et al. [9] used several color spaces to segment skin regions in the facial image in addition to Gaussian based methods. The method of segmenting face regions in the image using template matching technique is suggested in [16], [17], [19].

In this paper, a comprehensive study of three important issues of the color pixel classification approach to face

segmentation, namely selection of color spaces, classification algorithm and face detection are presented. Thirteen different color spaces and six different color pixel classification algorithms and one face detection algorithm are examined. To support this study, XM2VTS face database consisting of more than 100 color images together with manually prepared ground-truth for skin segmentation and face detection were used. The paper is organized as follows. Section II is devoted to different skin classifications techniques like color representations and color pixel classification algorithms. The face detection method using template matching technique is discussed in Section III. The results of our analysis and comparison are presented in Section IV, and conclusions are given in Section V.

## 2. SKIN SEGMENTATION

The aim of skin color pixel classification is to determine if a color pixel is a human skin color or non-skin color. Good skin color pixel classification should provide coverage of all different skin color types (blackish, yellowish, brownish, whitish.) and cater for as many different lighting conditions as possible. This section describes the color spaces and the classification algorithms that are investigated in this study.

### A. Color Spaces Used for Skin Segmentation

In the past, different color spaces have been used in skin segmentation. In some cases, color classification is done using only pixel chrominance because it is expected that skin segmentation may become more robust to lighting variations if pixel luminance is discarded. The choice of the color space is important for many computer vision algorithms. No color space can be considered as universal because color can be interpreted and modeled in different ways. This paper, investigates how the choice of color space and the use of chrominance channels affect skin

segmentation. There exist numerous color spaces but many of them share similar characteristics. Hence, in this study, thirteen color spaces which are commonly used in the image processing field are focused viz. RGB, YCbCr, YUV, YIQ, YEs, HSV, HSI, HLS, HCI, Normalized RGB, CIE-Lab, CIE-Luv and UCS. The description about the different color spaces specified here are discussed in addition to the color conversion techniques in the next section.

### B. Skin Conversions

RGB (Red Green Blue) color space is an additive color system based on tri-chromatic theory. Often found in systems that use a CRT to display images. RGB color space is easy to implement but non-linear with visual perception. It is device dependent and specification of colors is semi-intuitive. RGB is very common, being used in virtually every computer system as well as television, video etc. The RGB model is usually represented by a unit cube with one corner located at the origin of a three-dimensional color coordinate system, the axes being labeled R, G, B, and having a range of values  $[0, 1]$ . The origin (0, 0, 0) is considered black and the diagonally opposite corner (1, 1, 1) is called white. The line joining black to white represents a gray scale and has equal components of R, G, B [14].

YCrCb is an encoded nonlinear RGB signal, commonly used by European television studios and for image compression work. Color is represented by luminance, constructed as a weighted sum of the RGB values, and two color difference values Cr and Cb that are formed by subtracting luminance from RGB red and blue components. Y is the luminance information.

$$Y = 0.299R + 0.587G + 0.114B$$

$$Cr = R - Y \quad (1)$$

$$Cb = B - Y$$

The YUV model defines a color space in terms of one luminance and two chrominance components. The YUV color model is used in the PAL, NTSC, and SECAM composite color video standards. Previous black-and-white systems used only luminance (Y) information and color information (U and V) was added so that a black-and-white receiver would still be able to display a color picture as a normal black and white pictures.

YUV models human perception of color more closely than the standard RGB model used in computer graphics hardware. Y stands for the luma component (the brightness) and U and V are the chrominance (color) components. The YPbPr color model used in analog component video and its digital child YCbCr used in digital video are more or less derived from it (Cb/Pb and Cr/Pr are deviations from grey on blue-yellow and red-cyan axes whereas U and V are blue-luminance and red-luminance differences), and are sometimes inaccurately called "YUV".

$$\begin{aligned} Y &= 0.299R + 0.587G + 0.114B \\ U &= -0.147R - 0.289G + 0.437B \\ V &= 0.615R - 0.515G - 0.100B \end{aligned} \quad (2)$$

YIQ color model was designed to separate chrominance from luminance. This was a requirement in the early days of color television when black-and-white sets still were expected to pick up and display what were originally color pictures. The Y-channel contains luminance information which is sufficient for black-and-white television sets while the I and Q channels (in-phase and in-quadrature) carried the color information. A color television set would take these three channels, Y, I, and Q, and map the information back to R, G, and B levels for display on a screen.

$$\begin{aligned} Y &= 0.30R + 0.59G + 0.11B \\ I &= 0.60R - 0.28G + 0.31B \\ Q &= 0.21R - 0.51G + 0.31B \end{aligned} \quad (3)$$

The YIQ system is the color primary system adopted by National Television System Committee (NTSC) for color TV broadcasting. The YIQ color solid is made by a linear transformation of the RGB cube. Its purpose is to exploit certain characteristics of the human eye to maximize the utilization of a fixed bandwidth. The human visual system is more sensitive to changes in luminance than to changes in hue or saturation, and thus a wider bandwidth should be dedicated to luminance than to color information. Y is similar to perceived luminance; I and Q carry color information and some luminance information.

The corresponding transformation from RGB color model to YES color model is given below:

$$\begin{aligned} Y &= 0.253R + 0.684G + 0.063B \\ E &= 0.500R - 0.500B + 0.000B \\ S &= 0.250R + 0.250G - 0.500B \end{aligned} \quad (4)$$

The transformation simplicity and explicit separation of luminance and chrominance components makes this color space attractive for skin color modeling.

Hue-saturation based color spaces were introduced when there was a need for the user to specify color properties numerically. They describe color with intuitive values, based on the artist's idea of tint, saturation and tone. Hue defines the dominant color (such as red, green, purple and yellow) of an area; saturation measures the colorfulness of an area in proportion to its brightness. The "intensity", "lightness" or "value" is related to the color luminance. The intuitiveness of the color space components and explicit discrimination between luminance and chrominance properties made these color spaces popular in the works on skin color segmentation.

However, points out several undesirable features of these color spaces, including hue discontinuities and the computation of "brightness" (lightness, value), which conflicts badly with the properties of color vision.

Thus by means of the above equation one can be able to detect the skin regions from HSV images.

$$\begin{aligned}
 H &= \arccos \frac{\frac{1}{2}((R-G) + (R-B))}{\sqrt{((R-G)^2 + (R-B)(G-B))}} \\
 S &= 1 - 3 \frac{\min(R, G, B)}{R + G + B} \\
 V &= \frac{1}{3}(R + G + B)
 \end{aligned} \tag{5}$$

The HSI color space is very important and attractive color model for image processing applications because it represents colors similarly how the human eye senses colors. The HSI color model represents every color with three components: hue ( H ), saturation ( S ), intensity ( I ). The HSI color space (hue, saturation and intensity) attempts to produce a more intuitive representation of color. The I axis represents the luminance information. The H and S axes are polar coordinates on the plane orthogonal to I.

$$\begin{aligned}
 I_1 &= (R + G + B) / 3 \\
 I_2 &= (R - B) / 2 \\
 I_3 &= (2 * G - R - B) / 4 \tag{6} \\
 I &= I_1 \\
 S &= \text{SQRT}(I_1^2 + I_3^2) \\
 H &= \text{atan}(I_3 / I_2)
 \end{aligned}$$

H is the angle, specified such that red is at zero, green at 120 degrees, and blue at 240 degrees. Hue thus represents what humans implicitly understand as color. S is the magnitude of the color vector projected in the plane

orthogonal to I, and so represents the difference between pastel colors (low saturation) and vibrant colors (high saturation). The main drawback of this color space is that hue is undefined if saturation is zero, making error propagation in transformations from the RGB color space more complicated.

The HSL color space, also called HLS or HSI, stands for Hue, Saturation, Lightness (also Luminance or Luminosity) / Intensity. HSL does not define colors exactly because, like RGB, it is not an absolute color space. Since the color of RGB depends on the exact shade of red, blue and green ("primaries") used, so HSL, which is a simple transformation of RGB, also depends on the primaries.

Normalized RGB is a representation that is easily obtained from the RGB values by a simple normalization procedure:

$$\begin{aligned}
 r &= \frac{R}{(R + G + B)} \\
 g &= \frac{G}{(R + G + B)} \\
 b &= \frac{B}{(R + G + B)}
 \end{aligned} \tag{7}$$

As the sum of the three normalized components is known (r+g+b=1), the third component does not hold any significant information and can be omitted, reducing the space dimensionality. The remaining components are often called "pure colors", for the dependence of r and g on the brightness of the source RGB color is diminished by the normalization. A remarkable property of this representation is that for matte surfaces, while ignoring ambient light, Normalized RGB is invariant (under certain

assumptions) to changes of surface orientation relatively to the light source

CIE Lab color space is a color-opponent space with dimension L for luminance and a and b for the color-opponent dimensions, based on nonlinearly-compressed CIE XYZ color space coordinates. The coordinates of the Hunter 1948 L, a, b color space are L, a, and b. However, Lab is now more often used as an informal abbreviation for the CIE 1976 L\*a\*b\* color space (also called CIELAB, whose coordinates are actually L\*, a\*, and b\*). CIELAB is the second of two systems adopted by CIE in 1976 as models that better showed uniform color spacing in their values. CIELAB is an opponent color system based on the earlier (1942) system of Richard Hunter called L, a, b. Color opposition correlates with discoveries in the mid-1960s that somewhere between the optical nerve and the brain, retinal color stimuli are translated into distinctions between light and dark, red and green, and blue and yellow. CIELAB indicates these values with three axes: L\*, a\*, and b\*. The central vertical axis represents lightness (signified as L\*) whose values run from 0 (black) to 100 (white). This scale is closely related to Munsell's value axis except that the value of each step is much greater. This is the same lightness valuation used in CIE-LUV[13], [14]. A new color space, YCgCr, is described and applied for face detection. Although similar to the YCbCr color space, it differs in the use of the Cg color component instead of the Cb one. Here, the fundamentals of this new color space YCgCr are presented [15].

$$\begin{aligned}
 Y &= (0.256 * R) + (0.502 * G) + (0.096 * B) + 16 \\
 Cb &= (-0.317 * R) + (0.438 * G) - (0.121 * B) + 128 \quad (8) \\
 Cg &= (0.438 * R) - (0.366 * G) - (0.071 * B) + 128
 \end{aligned}$$

### C. Skin Classification Algorithms

Several algorithms have been proposed for skin color pixel classification. They include piecewise linear classifiers [4],[5],[6],[7], the Bayesian classifier with the histogram technique [9], [10], and Gaussian classifiers [8], [9]. The decision boundaries of these classifiers range from simple shapes (e.g., rectangle and ellipse) to more complex parametric and nonparametric forms.

#### 1. Piecewise Linear Decision Boundary Classifiers

In this category of classifiers, skin and non-skin colors are separated using a piecewise linear decision boundary. Mei-Juan Chen [4] used YCbCr color space to detect skin color. Sobottka and Pitas [5] proposed a set of fixed skin thresholds in the HS plane. Jure Kovac [6] used RGB color space to detect face region in 2D and 3D color spaces. Teodorescu [7] used normalized RGB color space to segment face region in color images. These approaches are based on the observation that skin chrominance, even across different skin types, has a small range, whereas skin luminance varies widely. In this study, thirteen color spaces which are commonly used in the image processing field are focused viz. RGB, YCbCr, YUV, YIQ, YES, HSV, HSI, HLS, HCl, n-rgb, CIE-Lab, CIE-Luv and UCS. The skin pixel classification conditions are shown in the table 1.

#### 2. Bayesian Classifier with the Histogram Technique

The Bayesian decision rule for minimum cost is a well-established technique in statistical pattern classification [9], [10]. Using this decision rule, a color pixel x is considered as a skin pixel if

$$\frac{p(x / skin)}{p(x / nonskin)} \geq \tau \quad (9)$$

where  $p(x/skin)$  and  $p(x/nonskin)$  are the respective class-conditional probability density functions of skin and non-skin colors and  $t$  is a threshold. The theoretical value of  $t$  that minimizes the total classification cost depends on the a priori probabilities of skin and non-skin and various classification costs. However, in practice  $t$  is often determined empirically. The class-conditional probability density functions can be estimated using histogram or parametric density estimation techniques.

### 3. Gaussian Classifiers

Terrillon et al. [8] compared Gaussian and Gaussian mixture models across nine chrominance spaces. Phung et al. [9] used eight color spaces to segment skin regions in the facial image in addition to Bayesian based and Gaussian based methods. The Bayesian classifier with the histogram technique has been used for skin detection by Jones and Rehg [10], [11]. The class-conditional probability density function of skin colors is approximated by a parametric functional form, which is usually chosen to be a unimodal Gaussian, or a mixture of Gaussians [9]. In the case of the unimodal Gaussian model, the skin class conditional probability density function has the form:

$$p(x/skin) = g(x; m_s, C_s) = 2\pi^{-d/2} |C_s|^{-1/2} \exp[-1/2(x - m_s)^T C_s^{-1} (x - m_s)] \quad (10)$$

where  $d$  is the dimension of the feature vector,  $m_s$  is the mean vector and  $C_s$  is the covariance matrix of the skin class. If we assume that the non-skin class is uniformly distributed, the Bayesian rule in (10) reduces to the following: a color pixel  $x$  is considered as a skin pixel if

$$(x - m_s)^T C_s^{-1} (x - m_s) \leq \tau \quad (11)$$

where  $\tau$  is a threshold and the left hand side is the squared Mahalanobis distance. The resulting decision boundary

is an ellipse in 2D space and an ellipsoid in 3D space. In this study, we also investigate the approach of modeling both skin and non-skin distributions as unimodal Gaussians. In this case, it can easily be shown that  $x$  is a skin pixel if

$$(x - m_s)^T C_s^{-1} (x - m_s) - (x - m_{ns})^T C_{ns}^{-1} (x - m_{ns}) \leq \tau \quad (12)$$

where  $\tau$  is a threshold and  $m_{ns}$  and  $C_{ns}$  are the mean and the covariance of the non-skin class, respectively. Another approach is to model both skin and non-skin distributions as Gaussian mixtures [9], [11]:

$$p(x/skin) = \sum_{s,i} s_{s,i} g(x; m_{s,i}, C_{s,i}) \quad (13)$$

$$p(x/nonskin) = \sum_{ns,i} ns_{ns,i} g(x; m_{ns,i}, C_{ns,i}) \quad (14)$$

The parameters of a Gaussian mixture (i.e., weights, means  $m$ , covariance  $C$ ) are typically found using the Expectation/Maximization algorithm.

### 3. FACE DETECTION

The algorithms mentioned earlier segment a skin region. But a skin region is assumed to be a face region if a skin region has at least one hole in it and that region is processed to locate a face. Otherwise the region is ignored. There are more than one hole in a human face in the form of two eyes, two nozzles, and ears. For the side view images there may be more than one hole in the form of one eye and one ear.

In order to find the number of skin regions in the given image the regions must be labeled. Labeling such regions does the process of determining the number of human skin regions in a binary image. A label is an integer value. An 8-connected neighborhood is used in order to determine the labeling of a pixel. If any of the neighbor pixels had a label, the current pixel is labeled with that label. If not, then a new label is used. At the end, the number of labels is counted in the segmented image and this will be the number of regions.

To separate each of these skin regions, the image is scanned and a new image is created that will have ones in the positions where the label occurs. The others are set to zero. This process is repeated for each of the skin regions found in order to determine if the skin region corresponds to a frontal human face or not.

**A. Number of Holes Inside A Region**

At this step it is necessary to find which the regions have at least one hole inside it. The regions without holes are ignored. Number of holes in a region can be calculated by using Euler number [16] [17]:

$$E = C - H \tag{15}$$

where

E : The Euler number

C : The number of connected components

H : The number of holes in a region.

For our case, the number of connected components is set to 1 since one skin region will be considered at a time. The number of holes is, then:

$$H = 1 - E \tag{16}$$

where

H : The number of holes in a region

E : The Euler number

When a hole is found in a region, the region is assumed to contain a face. Before searching, some information about the region is needed to make the classification.

**B. Center of Mass**

In order to study the region, its area and center of the region must be determined. The center of the area in binary image is the same as the center of the mass and is computed as shown below:

$$\bar{X} = (1/A) * \sum_{i=1}^n \sum_{j=1}^n j * B[i, j] \tag{17}$$

$$\bar{Y} = (1/A) * \sum_{i=1}^n \sum_{j=1}^n i * B[i, j] \tag{18}$$

where:

A : The area in pixels of the region

B : The matrix of size [n x m] representation of the region

**C. Orientation**

Most of the faces are vertically oriented. However some of them have little inclination. If the template face is rotated in the right angle, there will be higher matching. The orientation of the axis of the elongation will determine the orientation of the region. In this axis the inertia will be the minimum.

The axis is computed by finding the line for which the sum of the squared distances between region points and the line is the minimum. The angle of inclination is

$$\text{given by: } \theta = (1/2) \text{atan}(b/(a-c)) \tag{19}$$

where

$$a = \sum_{i=1}^n \sum_{j=1}^m (x'_{ij})^2 B[i,j] \tag{20}$$

$$b = 2 \sum_{i=1}^n \sum_{j=1}^m (x'_{ij})(y'_{ij})(B[i,j]) \tag{21}$$

$$c = \sum_{i=1}^n \sum_{j=1}^m (y'_{ij})^2 B[i,j] \tag{22}$$

$$x' = x - \bar{x}$$

$$y' = y - \bar{y}$$

**D. Width and Height Of The Region**

First, the region with holes is filled out. This is to avoid problems when holes are encountered. Now it is necessary to determine the height and width by moving 4 pointers: one from the left, right, top and bottom of the

image. If a pixel is found with a value other than 0, the pointer is stopped and this is the coordinate of a boundary. With the help of the 4 values, the height of the facial region is computed by subtracting the bottom and top values and the width is computed by subtracting the right and the left values.

### E. Region Ratio

The width and the height of the region are used to improve the decision process. The height to width ratio of the human faces is around 1. In order to have less misses however, it is found that a minimum good value is 0.8. Ratio values below 0.8 do not suggest a face since human faces are oriented vertically.

The ratio should also have an upper limit. This is determined by analyzing the results in our experiments that a good upper limit should be around 1.6.

While the above-mentioned information improves the classification, it can also be a drawback for cases such as the arms that are very long. If the skin region for the arms has holes near the top, this might yield into a false classification.

### F. Template Matching

One of the most important characteristics of this method is that it uses a human face template to take the final decision of determining if a skin region represents a face. The template is chosen by averaging 16 frontal view faces of males and females wearing no glasses and having no facial hair. The template used is shown in figure 1. Notice that the left and right borders of the template are located at the center of the left and right ears of the averaged faces. The template is also vertically centered at the tip of the nose of the model. At this point, all the required parameters are available to do the

matching between the part of the image corresponding to the skin region and the template human face. For the image corresponding to the skin region, the holes in the region are closed and this image is multiplied with the original one.

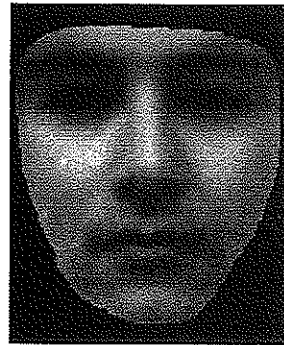


**Figure 1: Template Face (Model) Used To Verify The Existence Of Faces In Skin Regions**

The template face has to be positioned and rotated in the same coordinates as the skin regions image. The template face is resized according to the height and the width of the region of the region computed. The resized template face is rotated to  $-\theta$ , so that it is aligned in the same direction as the skin region. The center of the rotated template face is computed. Then the cross-correlation between the part of the image corresponding to the skin region and the template face is computed. After the system decided that the skin region is a frontal human face, we get a new image with a hole exactly the size and shape of that of the processed template face. The pixel values of this image are inverted to generate a new one, which, multiplied by the original grayscale image, will yield an image as the original one, but with the template face located in the selected skin region.



The coordinates of the frontal face image are determined and a rectangle is drawn in the original color image [16], [17], [18]. The figure 2 shows the algorithm for the face detection system.

## 5. CONCLUSIONS

An analysis of the pixel-wise skin segmentation approach that uses color pixel classification is presented. The 2D unimodal Gaussian classifier with the histogram technique classifier had a maximum CDR of 99.10 percent. But the Bayesian classifier produces best results with 99.43 percent. The piecewise linear classifiers applied for HSV and RGB color spaces produces still higher classification rates than all other classifiers for image with good illumination conditions. The comparative study based on the Bayesian classifier shows that pixel-wise skin segmentation is largely unaffected by the choice of color space. However, segmentation performance degrades if only chrominance channels are used and there are significant performance variations between different choices of chrominance. All the classifiers can successfully identify exposed skin regions including face, hands, and neck. However, objects in the background with similar colors as the skin will invariably lead to false detections, hence the need for post processing steps. The skin segmented image is post processed for face detection using the shape based model.

## 6. EXPERIMENTAL RESULTS

A comprehensive set of experiments were performed to analyze the effects of color space selection on human skin segmentation and to compare different classification algorithms. The algorithm proposed in this paper is used to detect human faces in the color images. It produces best results when the images taken from better lighting conditions are used. But if the images with complex background are used, better results are obtained. The image sources are too numerous to list here but they were chosen to ensure the diversity in terms of the

background scenes, lighting conditions, and face and skin types. The lighting conditions include indoor lighting and outdoor lighting; the skin types include whitish, brownish, yellowish, and darkish skins. The ground-truth images were meticulously prepared by manually segmenting the face and skin regions. The skin segmented images consist of all exposed skin regions such as facial skin, neck, arms, and hands.

The segmentation performance was measured in terms of the correct detection rate (CDR) and the false detection rate (FDR) is shown in the table III. The CDR is the percentage of skin pixels correctly classified; the FDR is the percentage of non-skin pixels incorrectly classified.

In our study, thirteen skin color pixel classifiers were compared. For the six piecewise linear classifiers, we took the fixed parameters directly from the original references [8], [10]. For the Gaussian mixture classifier, we used the model parameters published by Jones and Rehg [5]. thirteen different color spaces are used with three Gaussian classifiers were tested: a 2D unimodal Gaussian classifier, a 3D unimodal Gaussian classifier, and mixture of Gaussian classifiers using the YCbCr, HSV, RGB, CIE Lab, Normalized rgb and HSI color spaces. For the Bayesian classifier with the histogram technique, we used the YCbCr, HSV, RGB, CIE Lab, Normalized RGB and HSI color spaces and histograms with 2563 bins. The 2D unimodal Gaussian classifier with the histogram technique produces good results with a maximum CDR of 99.10 percent. But the Bayesian classifier produces best results with 99.43 percent. The piecewise linear classifiers applied for RGB produces still higher classification rates than all other classifiers for images with good illumination conditions. The template matching technique is used to mark facial region in the image. The comparative performance of the face detection using template matching technique is shown in the table I. A small portion of the sample outputs are shown in figure 3.

## Face Detection In Color Images Using Pixel Based Skin Color Detection Techniques

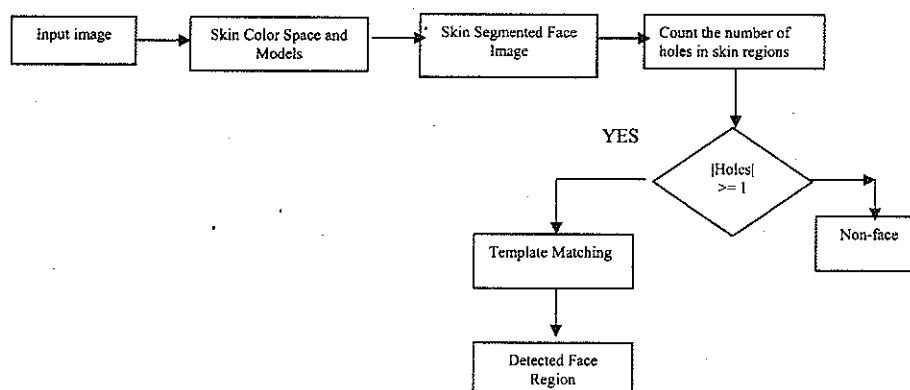


**Figure 2 : The face Detection Algorithm using Template Matching**

**Table : 1 Piecewise Linear Decision Boundary Classifiers for Skin Detection**

HSV	RGB	HIS	YCbCr	nRGB	CIE Lab
H: 0.40 -> 0.70	R > 95, G > 40, B > 20,	I: 0 -> 0.53	Cb: 77 -> 127	r: 0.31 -> 0.465	C: 0 -> 65
S : 0.15 -> 0.75	Max{R,G,B} - Min{R,G,B}	S: 13 -> 110	Cr: 133 -> 173	g: 0.27 -> 0.63	I: 0 -> 14
V: 0.35 -> 0.95	< 15,  R-G  > 15, R > G,	H: 0 -> 28			
	R > B				

**Table : 2 Correct Detection Rates**

Classification Algorithms		HSV	RGB	HIS	YCbCr	nRGB	CIE Lab
Piecewise Linear Classifiers		99.5495	100	67.3887	96.0770	94.9344	99.5492
Gaussian Classifiers	1	48.8902	79.7015	43.5272	99.1012	77.1081	70.7625
	2	48.8702	79.7019	42.5284	99.1017	77.1081	70.7645
	3	21.9034	98.1045	21.9021	57.6650	23.8716	47.9227
Bayesian Classifier		99.4264	96.6462	82.4044	97.0415	56.1324	98.6243

1 - 2D Unimodal

2 - Mixture of Gaussian

3 - 3D Unimodal Gaussian

**Table : 3 Results of The Face Detection**

Type of the Algorithm used	No. of face images used	No. of Images Detected	Missed Results	Percentage of the Correct Face Detection
With Template Matching	45	42	3	93%
Without Template Matching	45	40	5	89%

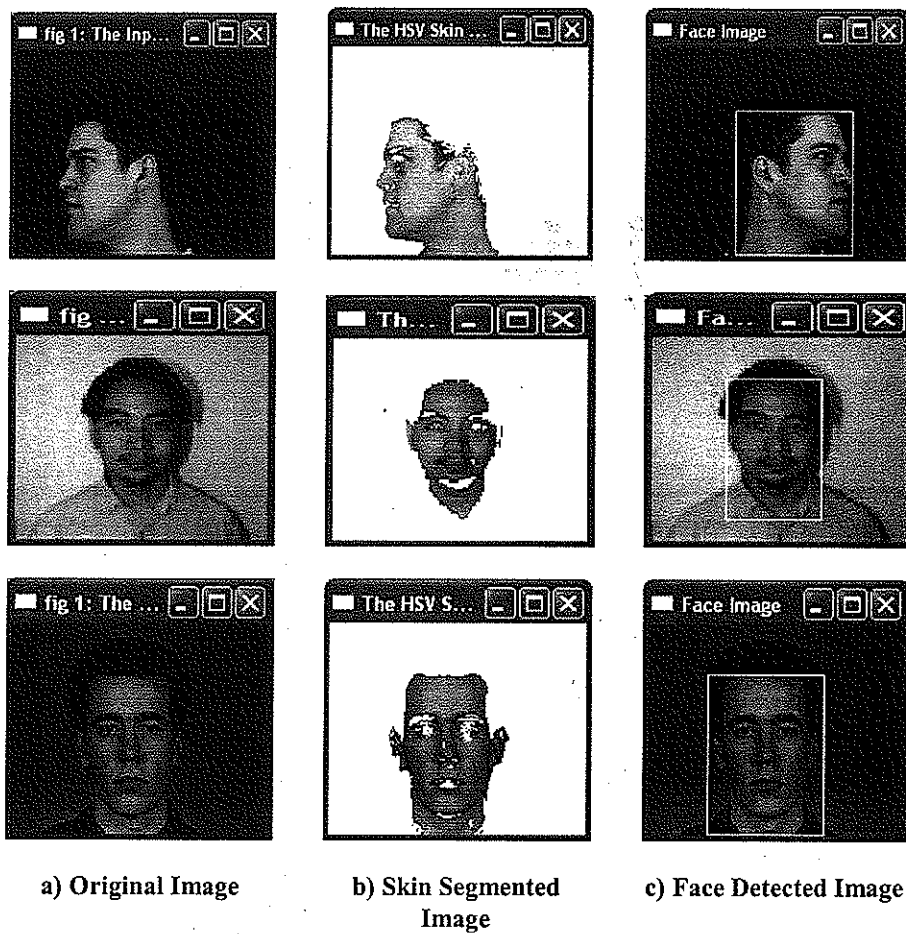


**Figure : 3 Sample Outputs**

## REFERENCES

- [1] R.L. Hsu, M. Abdel-Mottaleb and A.K. Jain, "Face Detection in Color Images", IEEE Trans. Pattern Analysis and Machine Intelligence, Vol. 24, No. 5, PP. 696-707, May 2002.
- [2] M.H. Yang, D. Kriegman, N. Ahuja, "Detecting Faces in Images : A Survey", IEEE Trans. Pattern Analysis and Machine Intelligence, Vol. 24, No.1, Jan. 2002.
- [3] Eric Hjelmas, Boon Kee Low, "Face Detection : A Survey ", Computer Vision and Understanding, Vol 83, PP. 236-274, 2001.
- [4] Mei-Juan Chen, Ming-Chieh Chi, Ching-Ting Hsu, Jeng-Wei Chen, "ROI Video Coding Based on H.263+ with Robust Skin-Color Detection Technique", IEEE Trans. Consumer Electronics, Vol.49, No.3, Aug 2003.
- [5] K. Sobottka and I. Pitas, "A Novel Method for Automatic Face Segmentation, Facial Feature Extraction and Tracking", Signal Processing: Image Comm., Vol. 12, No. 3, PP. 263-281, 1998.
- [6] Jure Kovac, Peter Peer, France Solina, "2D Versus 3D Color Space Face Detection", Proc. 4th EURASIP Conf. on Video/ Image Processing and Multimedia Communications, Zagreb, Croatia, PP. 2-5, July 2003.
- [7] T.D. Teodorescu, V.A. Maiorescu, J.L. Nagel, M. Ansorge, "Two color. Based Face Detection Algorithms: A Comparative Approach", Proc. IEEE Conf. Vol. 0, PP. 7803-7979, Sep. 2003.
- [8] J.C. Terrillon, M.N. Shirazi, H. Fukamachi and S. Akamatsu, "Comparative Performance of Different Skin Chrominance Models and Chrominance Spaces for the Automatic Detection of Human Faces in Color Images", Proc. IEEE Int'l Conf. Automatic Face and Gesture Recognition, PP. 54-61, Mar. 2000.
- [9] S.L. Phung, A. Botuzerdounm and D. Chai, "Skin Segmentation Using Color Pixel Classification: Analysis and Comparison", IEEE PAMI Vol. 27(1) PP. 148-154, Jan 2005.
- [10] J. Jones and J.M. Rehg, "Statistical Color Models with Application to Skin Detection", Int'l J. Computer Vision, Vol. 46, No. 1, PP. 81-96, Jan. 2002.
- [11] Krishnan Nallaperumal, Subban Ravi, C.K. Babu, et al, "Skin Detection using Color Pixel Classification with Application to Face Detection: A Comparative Study", Proc. ICCIMA International Conference on Computational Intelligence and Multimedia Applications, Vol. 3 PP. 436-441, December 2007.
- [12] Son Lam Phung, Abdeselem Bouserdoum, Douglas Chai, "Skin Segmentation Using Color And Edge Information", Proc. Int. Symposium on Signal Processing and its Applications. Vol.0, PP 7803-7946, 1-4 July 2003, Paris, France.
- [13] Adrian Ford, Alan Roberts, "Colour Space Conversions", A Technical Report.
- [14] Marko Tkalcic, Jurij. F. Tasic, "Colour spaces - perceptual, historical and applicational background", EUROCON 2003 Ljubljana, Slovenia, Dec. 2003.
- [15] Juan Jose' De Dios, Narciso Garcia, " Face Detection Based On A New Color Space YCgCr", In IEEE Conf., Aug. 2003, PP. 909-912. Aug 2003.
- [16] LI-Hong Zhao, Xiao-Lin Sun, Ji-Hong Liu, Xin-He Xu, "Face Detection Based on Skin Color", Proceedings of the Third International Conference

on Machine Learning and Cybernetics, Shanghai. Recognition, PP. 54-61, Mar. 2000.

[17] Krishnan Nallaperumal, Ravi Subban, et al, "*Human Face Detection in Color Images Using Skin Color and Template Matching Models for Multimedia on the Web*", IEEE Conf. On Wireless and Optical Communication Networks WOCN, Bangalore, India, 2006.

[18] Chang. H, and Robles. U, "*face Detection*", May 2000 <http://www-cs-tudents.stanford.edu/robles/ee368/>

[19] XM2VTS face database, <<http://xm2vtsdb.ee.surrey.ac.uk/home.html>>.

#### **Author's Biography**



**Ravi Subban** received B.E degree in Computer Science and Engineering from Bharathiar University, Coimbatore, India in 1989, M.Tech degree in Computer and Information Technology from Centre for Information Technology and Engineering, Manonmaniam Sundaranar University, Tirunelveli, in 2004. Currently, he is doing Ph. D in Computer Science and Engineering at Manonmaniam Sundaranar University Tirunelveli. He is working as a

Selection Grade Lecturer in the Centre for Information Technology and Engineering, Manonmaniam Sundaranar University, Tirunelveli. His research interests include Image Processing, Face detection and Machine Vision and Pattern Recognition. He has published 15 scientific papers in International Conference Proceedings and Journals. He is a Member of the IEEE.



**Nallaperumal Krishnan** received M.Sc. degree in Mathematics from Madurai Kamaraj University, Madurai, India in 1985, M.Tech degree in Computer and Information Sciences from Cochin University of Science and Technology, Kochi, India in 1988 and Ph.D. degree in Computer Science & Engineering from Manonmaniam Sundaranar University, Tirunelveli. Currently, he is heading department of Centre for Information Technology and Engineering of Manonmaniam Sundaranar University, Tirunelveli. His research interests include Signal and Image Processing, Remote Sensing, Visual Perception, Mathematical Morphology Fuzzy Logic and Pattern recognition. He has authored three books, edited 18 volumes and published 25 scientific papers in Journals. He is a Senior Member of the IEEE.